ISSN 0974 - 9373

Vol. 24 No. 2 (2020) **Journal of International Academy of Physical Sciences** pp. 191- 202

On the Diffraction and Line of Sight (Los) Centered Loss Modelling of VHF TV Signal over Hilly Terrain

Thaisa Jawhly and Ramesh Chandra Tiwari

Department of Physics
Mizoram University, Aizawl-796004, Mizoram, India
Email: thaisjly@gmail.com, ramesh_mzu@rediffmail.com

(Received May 07, 2020)

Abstract: This paper discusses the diffraction loss due to obstruction and its analysis based ona single knife-edge diffraction method to arrive at a precise loss estimate. We supplement this study with the measurement data of continuous-wave propagating at 182.25 MHz over variable hilly terrain. After calculating the measured signal,we used the loss exponent estimated from the measured signal in computing the loss for the obstructed region, which we add with the diffracted loss. The analysis showed that the recommendations of the ITU-R diffraction model give a good agreement with the measured data. We proposed apropagation loss model dependent on the diffraction and line of sight (LoS).

Keywords: single knife-edge diffraction loss, propagation loss, line of sight loss, terrestrial propagation.

1. Introduction

Precise estimation of signal variation across different propagation scenarios is a prerequisite for the proper deployment of a wireless communication system. A radio signal travels through scattering, reflection, and diffraction[1],and the received signal at the far end is an outcome of signal that traverses multiple paths. Due to the high cost of in-site measurement, radio engineers resort to using existing propagation loss models. These loss models provide an insight of signal variation before the actual deployment of the transmitter (Tx) across a given scenario.

Very High Frequency (VHF) signal frequencies range from 30 MHz to 300 MHz and are the main module of the terrestrial communication system.

This frequency band has numerous civilian and military applications.The advent of the Cognitive Radio Access (CRA)[2,3] network, and the Internet of Things (IoT)[4] administered the importance of wireless-based technology. And to facilitate the constant-increasing demand for wireless connectivity, a terrestrial communication system is still important regardless of advanced achievements in the field of communication engineering.

In wireless propagation analysis, the Okumura-Hata model is one renowned model often used as the referenced model. It is the result of vast empirical measurement over the quasi-smooth terrain made in Japan[5]. However, in different terrain settings, the same loss model needs augmentation for a clear-cut estimation of the loss predicted. As such, for the proper estimate of loss in mixed terrain settings, we need to model the loss based on the different channel affecting factors.

2. ITU Recommendations

Previous works have highlighted the success of implementing the International Telecommunication Recommendation in diverse wireless signal modeling[6-9]. Authors in[8] have reported a good agreement of ITU Rec-529 to the spectrallyaccelerated forward-backwards (FBSA) method. While the varying clutter terrain loss analysis in the forested region performed by authors in[7] has reported the success of implementing the ITUR Rec- P.526 and P.1812 for measurements made in Rio de Janeiro.Whereas authors in[9] have highlighted the better performance of the Cascade knife-edge (Rec-P.526 12) over the Delta Bullington method (Rec- P526 11) for implementation in their Artificial neural network model.

Notwithstanding the works as mentioned above, The ITU Rec-P.526-15 is projected explicitly for frequencies above 30 MHzwithdifferent estimation methods for assessing the effects of diffraction on signal propagation. The primary aim of this paper is the VHFband, and hence only the single knife-edge diffraction is considered.

3. Measurement Campaign

We performed the data measurement survey inAizawl, Mizoram,North-East India. The signal strength measurementarea is within a 20 km radial area taken along the four cardinal directions of the transmitter. The transmitter transmits a continuous wave (CW),which we measured with Anritsu Sitemaster (S332E) using the standard Anritsu dipole antenna.We considered the VHF band III signals with a carrier frequency of 182.25 MHz propagating from 32 m high antenna. The experimental set-up parameters are presented in Table.1.

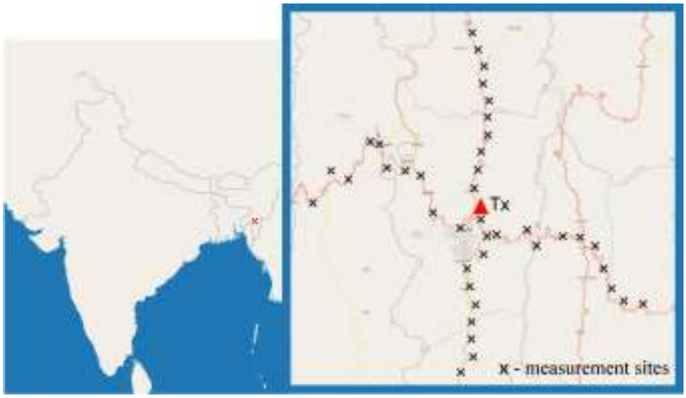

Figure 1. An aerial view of the study area (Aizawl Mizoram, India) with data collection points represented by 39 white cross marks. The red triangle represents the transmitter (Tx).

The total measurement data taken in 39 locations,consists of 20 sites obstructed by terrain. Out of the 20 sites, four sites have multiple terrain obstruction while the other 17 sites have single terrain obstructions. There are sixnon-line of sight (nLoS) sites with shadowing by tree canopy and buildings

Table 1 Measurement set-up parameters with their values and units

Parameters	**Values/units**
Transmitter height (hTx)	32 *m*
Mobile antenna height (hMx)	1.8 *m*
Frequency	182.25 MHz
Modulation	CW
Power transmitted (Pt)	30 dBw
Data collection points	39 locations
Mobile antenna type	Dipole antenna
Transmitter location coordinate	23.76, 92.73

4. **Theory and Method**

4.1 Knife-edge diffraction loss: In the non-line of sight (nLoS) scenario between Tx and Mx, the propagation loss increases dramatically. This loss due to obstruction from knife-edge diffraction is simplified and modeled as a function of only the Fresnel-Kirchoff parameter *v*.Wherewe calculate the Fresnel-Kirchoff diffraction parameter *v*using the relation given in[10].

(4.1) $$v = h\sqrt{\frac{2(d_1 + d_2)}{\lambda d_1 d_2}}$$

In the above equation, h is the effective height of the obstacle, d_1 is the distance between the peak of Tx and the obstacle while d_2 is the distance between the peak of Tx and Mx. λ is the wavelength of the signal transmitted. All the parameters are in meters.

(4.2) $$L = -20\log\left(\frac{\sqrt{[1 - \mathrm{c}(v) - \mathrm{s}(v)]^2 + [\mathrm{c}(v) - \mathrm{s}(v)]^2}}{2}\right),$$

where $c(v)$ and $s(v)$ are the complex Fresnel integral defined as

(4.3) $$c(v) + is(v) = \int_0^u e^{i\pi x^2/2}\,dx$$

$$= \int_0^u \cos\left(\tfrac{1}{2}\pi x^2\right)dx + i\int_0^u \sin\left(\tfrac{1}{2}\pi x^2\right)dx,$$

(4.4) $$c(v) = \int_0^u \cos\left(\tfrac{1}{2}\pi x^2\right)dx$$

We present the knife-edge diffraction loss as a function of Fresnel diffraction parameter *v*in Fig.2.
For *v*higher than -0.78 the value of *J*(*v*) in decibelis approximated as[11]

(4.5) $$J(v) = 6.9 + 20\log\left(\sqrt{(v-0.1)^2 + 1} + (v - 0.1)\right)dB.$$

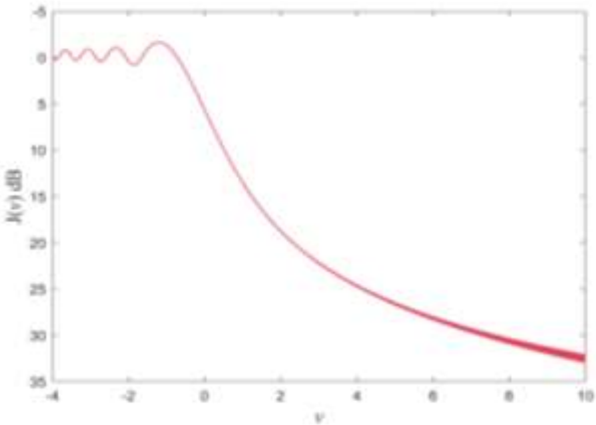

Figure 2. The plot is showing the variation of the knife-edge diffraction loss in decibel (dB) as a function of the diffraction parameter (v).

4.2 Determination of the effective height (h) of the knife-edge obstruction:

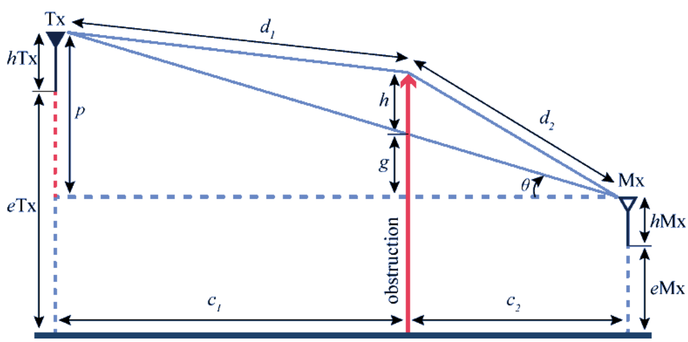

Figure 3. Illustration of the obstacle, transmitter (Tx), and mobile antenna (Mx) with their respective placement elevation *e*Tx and *e*Mx. We denote the effective height of the obstruction by *h*.

Owing to the hilly terrain region, the elevation (above sea level) for each measurement location (Mx location) is unique for different areas. The transmitter (Tx) is based on an elevation of 1385 m and stands 30 m above ground, while the measurement base of the mobile antenna (Mx) is at a different elevation (e_{Mx}). To make the calculation more accessible, we assume a ground level for Mx by subtracting e_{Mx} and h_{Mx} from h_{Tx} and e_{Tx}. First, we determined the elevation angle (θ) between Mx and Tx, and we obtained the perpendicular height g using a simple relationship $g = c_2 \tan\theta$. We calculate the effective height of the obstacle (h) by subtracting this g from the remaining obstruction height. The Fresnel diffraction parameter v calculated using c_1 and c_2 is practically similar to the value of v calculated using d_1 and d_2. However, to arrive at a precise estimate of v, we calculated d_1 and d_2 from the geometrical construction. Out of 21 obstructed sites, we evaluated 17 sites using single knife-edge diffraction, while we discarded 4 locations as they have multiple Tx-Mx obstructions.

4.3 Propagation losses: The total measured signal in $dBuV/m$, irrespective of the site location,is converted in dBw using the relation

(4.6) $$L = F + 20\log_{10}(\lambda A_r) \text{-} 156.75\, dBw$$

Using (4.6) the loss in decibel (dB) is computed using the relation

(4.7) $$Loss = Pt(dBw) - L(dBw) dB,$$

where F is the received signal strength in $dBuV/m$, λ is the wavelength, and A_r is the antenna gain ratio. For simplicity, we assume a unit antenna gain (antenna gain $= 0dBi$) for the mobile and transmitter antenna,where $A_r = 1$. The total power transmitted (in watt) is converted into dBw using the relation $dBw = 10\log_{10} Pt(\text{watt})$.

5. Loss analysis

5.1 Line of sight (LoS) loss: To determine the LoS loss, we employ the deterministic log-distance based model[12] expressed as

(5.1) $$L_{LOSn} = L_o + 10n\log_{10}\left(\frac{d}{d_0}\right)$$

In (5.1) L_O is the loss at reference distance $d_0 = 1$, where $L_o = 20\log_{10}(4\pi d_o/\lambda)$ while d is the distance between Tx and Mx in meter, and n is the loss exponent.

Table 2 Table showing the diffraction parameter, the mean diffraction loss evaluated at a different Tx–Mx separation (Rx), and the LoS loss combined with the diffraction loss (L_β).

Direction	Rx (km)	v	$J(v)$ (dB)	L_β(dB)
North	8.02	2.44	20.66	117.99
	15.99	6.15	28.61	125.69
	10.06	0.82	12.73	120.52
	12.04	2.93	22.21	122.53
	13.94	4.48	25.86	124.16
South	1.98	5.35	27.40	102.40
	7.99	4.49	25.89	117.95
	18.03	1.88	18.54	127.03
	19.99	0.89	13.20	128.19
	10.01	3.97	24.82	120.47
East	13.99	2.00	19.03	124.21
	15.97	9.70	32.59	125.68
West	18.21	0.04	6.39	127.14
	19.97	6.75	29.43	128.17
	9.93	1.49	16.73	120.38
	4.06	2.49	20.84	110.39
	19.99	1.94	18.80	122.49

Usually, the path loss exponent is $n = 2$ for free space. However, this can vary from 2.5 to 3.5 for suburban and urban environments[13]. For our measurement data, the line of sight (LoS) loss analysis showed that the loss exponent with a reference distance $d_0 = 1$ is 2.57.

We classified the distribution of the loss evaluated based on the LoS, Shadowed region, Single edge diffraction, and Multiple edge diffraction. We computed a separate theoretical LoS loss using (5.1) with $n = 2.57$ as mentioned above; however, we did not analyzethe multiple knife-edge diffraction (MKED) and the shadowing loss,individually as the SNED losses.We calculate these losses using (4.7) similar to the total data.These shadowed regions are the measurement sites not obstructed by terrain but obstructed by tree canopy and buildings.

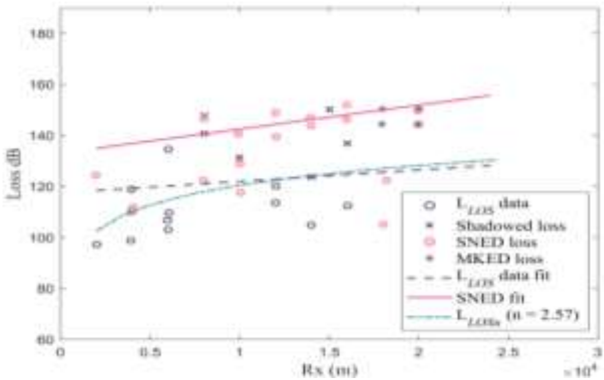

Figure 4. The plot is showing the mean line of sight (LoS) loss, Shadowed loss, Single knife-edge (SNED), Multiple knife-edge (MKED) loss with the LoS with loss exponent, n=2.57.

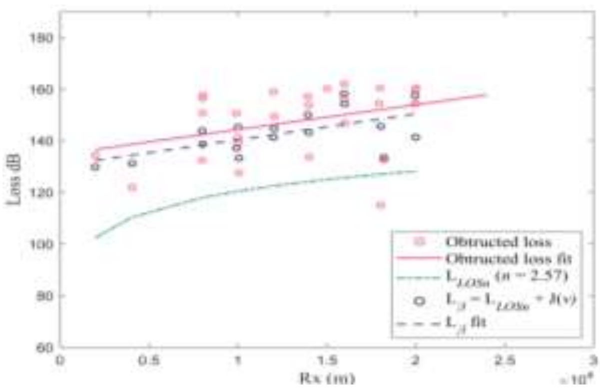

Figure 5. Comparison of the mean obstructed loss and the loss combination of the L_{LOSn} with the diffracted loss (L_{β}). The two straight-line fit the obstructed loss, and L_{β} has a difference of 3.4 dB.

The loss analysis showed that MKED loss and the shadowed loss projections are analogous to the SNED loss, as shown in Fig. 4And as such, we linked these loss data with the SNED loss data and designated them as the obstruction loss, as there is no clear-cut boundary between them. Furthermore, we separated the line of sight (LoS) signal measurement from the obstructed sites.

5.2 Diffraction loss: The diffraction loss computed using (4.6) shows a loss ranging from $6.3dB$ to $32.5dB$, as presented in Table.1. We learned that the total diffraction loss combined with the LoS loss corresponding with loss exponent ($n = 2.57$) is equivalent to the obstructed loss with minor

differences. This loss projected combining the LoS loss (L_{LOSn}) and the obstruction loss has an error of 3.4 dB less based on the least square fitting line, as shown in Fig.5.
Thus, we can deduce the diffraction loss based on this SNED analysis, whichwe expressed as

(5.2) $$L_\beta = L_{LOSn} + J(v) + \varepsilon ,$$

where L_{LOSn} is the LoS loss given in (4.7) and the $J(v)$ is the knife-edge diffracted loss calculated using (4.6) and ε is the required correction factor in dB.

We obtained the plot of the diffraction loss based on (5.2), without the correction factor and compared this with the fit of the measured loss data. We observed that even without including the correction factor, the line fit (L_β fit) shows a comparable fit with the obstructed loss.

6. Results

6.1 Proposed model: The calculated mean of the SNED loss is $21.39dB$, with a standard deviation of $6.8dB$. As mentioned earlier, we did not compute the diffraction loss for four locations due to MKED loss and the six areas shadowing loss. Since the graphical analysis showed a similar estimate, we assign the mean value of SNED losses to these ten sites (obstructed sites). Based on the above reviewif we mapped the LoS measurement site the value $\tau_{Loss} = 1$ and 0 otherwise, we can express the total measured loss as

(6.1) $$L(dB) = \tau_{LOS}(L_{LOSn}) + (1 - \tau_{LOS})L_\beta .$$

The above equation means that for every LoS site, the second term will reduce to zero, and for every nLoS site, the first term will reduce to zero, retaining only the second term. We calculated the correlation coefficient (r) using the relationship[14]

(6.2) $$r = \frac{\sum (X - \bar{X})(Y - \bar{Y})}{\sqrt{\sum (X - \bar{X})^2}\sqrt{\sum (Y - \bar{Y})^2}} .$$

In the above equation $\bar{X}$ and $\bar{Y}$ are the mean of the measured loss and the proposed loss, respectively.

The correlation coefficient and analysis indicated a strong positive relationship between the loss predicted using (6.1) and the measured data ($r = 0.79$). The corresponding r-squared ($\mathbb{R}^2$) computed value is 0.62, which indicated that the proposed loss explained 62 % of the total loss measured. We obtain regression of the proposed loss with the actual loss measured as shown in Fig. 6

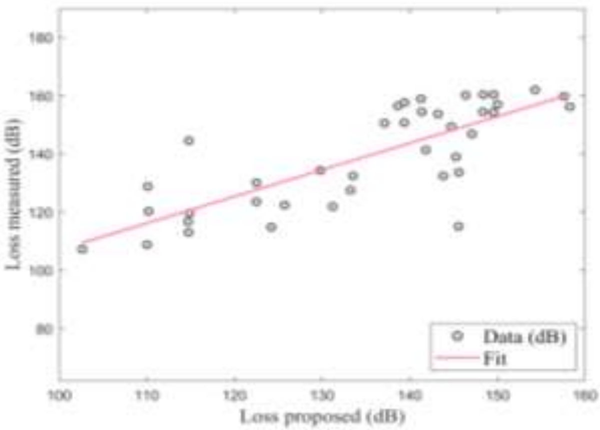

Figure 6. Regression plot of the proposed loss model with the mean measurement loss. A linear fit line indicates an $\mathbb{R}^2$ value of 0.62 with an *RMSE* of 10.9.

7. Conclusion

This work presents an analysis of single knife-edge diffraction loss over the hilly terrain region of Mizoram across the different scenarios. We took a reference measurement survey in 39 locations extending 20 km radial distance within the four cardinal directions of the transmitter. There are seventeensingle terrainobstructed sites out of the total measurement location. The LoS loss was calculated separately for the obstructed regions using the loss exponent deduced from measurement LoS data. We supplement this resultto the diffraction loss calculated, giving the total loss due to obstruction. The analysis showed that the ITU recommendation P.526-15 gives a good agreement with the measured loss. The proposed model could is applicable in any scenario with single terrain obstructed sites.

Acknowledgment: This research is supported by the National Fellowship and Scholarship for Higher Education of ST Students (NFST)(Award No:201718-NFST-MIZ-00476), Ministry of Tribal Affairs, Government of India. A Ph.D. Fellowship was awarded to the first author

References

1. Y. Zhang, L. Chu, S. Lee, T. Zhang, T. Yamazaki and H. Fukuda, Fast Prediction of RF Propagation Loss in Industrial Environments, *IEEE Int. Conf. Emerg. Technol. Fact. Autom. ETFA*, **2019** (2019), 1346–1350.
2. I. Kakalou, K. Psannis, P. Krawiec and R. Badea, Cognitive Radio Network and Network Service Chaining towards 5G : challenges and requirements, *IEEE Wireless Communications*, **22(6)** (2015), 34-39
3. Z. Zhao, M. C. Vuran D. Batur and E. Ekici, Shades of White: Impacts of Population Dynamics and TV Viewership on Available TV Spectrum, *IEEE Trans. Veh. Technol.*, **68(3)** (2019), 2427-2442.
4. T. Wei, W. Feng, Y. Chen, C.-X. Wang, N. Ge and J. Lu, Hybrid Satellite-Terrestrial Communication Networks for the Maritime Internet of Things: Key Technologies, Opportunities, and Challenges, (2019), 1–23.
5. T. Jawhly and R. C. Tiwari, Characterization of Path Loss for VHF Terrestrial Band in Aizawl, Mizoram (India), *Lecture Notes in Electrical Engineering*, (2019), 53–63
6. A. L. Penteado Botelho, Comparison of Propagation Models using Propagation Features, *Set Int. J. Broadcast Eng.*, **2019(1)** (2019), 63–72.
7. F. M. da Costa, L. A. R. Ramirez and M. H. C. Dias, Analysis Of ITU-R VHF/UHF Propagation Prediction Methods Performance on Irregular Terrains Covered by Forest, *IET Microwaves, Antennas Propag.*, **12(8)** (2018), 1450–1455.
8. C. A. Tunc, A. Altintas and V. B. Ertürk, Examination of Existent Propagation Models Over Large Inhomogeneous Terrain Profiles using Fast Integral Equation Solution, *IEEE Trans. Antennas Propag.*, **53(9)** (2005), 3080-3083.
9. G. P. Ferreira, L. J. Matos and J. M. M. Silva, Improvement of Outdoor Signal Strength Prediction in UHF Band by Artificial Neural Network, *IEEE Trans. Antennas Propag.*, **64(12)** (2016), 5404–5410.
10. I. Rashdan, F. De Ponte Muller, T. Jost, S. Sand and G. Caire, Large-Scale Fading Characteristics and Models for Vehicle-to-Pedestrian Channel at 5-Ghz, *IEEE Access*, **7** (2019), 107648–107658.
11. ITU-R, *Propagation by Diffraction*, Recommendation ITU-R P.526-15, 10/2019.
12. S. Kurt and B. Tavli, Path-Loss Modeling for Wireless Sensor Networks, *IEEE ANTENNAS Propag. Mag.*, **16** (2017), 2877-2880.

13. H. F. Ates, S. M. Hashir, T. Baykas and B. K. Gunturk, Path Loss Exponent and Shadowing Factor Prediction From Satellite Images Using Deep Learning, *IEEE Access*, **7** (2019), 101366–101375.

14. E. Kasuya, On the use of R and R Squared in Correlation and Regression, *Ecological Research*, (2018), 235-236.